Chromophore-Specific Quenching of Ruthenium Trisbipyridine−Arene Bichromophores by Methyl Viologen

Gerard J. Wilson,* Anton Launikonis, Wolfgang H. F. Sasse, and Albert W.-H. Mau

CSIRO, Division of Molecular Science, Private Bag 10, Rosebank MDC, Clayton, Victoria 3169, Australia

Received: October 6, 1997; In Final Form: February 25, 1998

The quenching (η_q) and subsequent cage-escape efficiency (η_{ce}) have been measured for three arene-linked ruthenium trisbipyridine complexes quenched by methyl viologen (MV^{2+}). The bichromophoric complexes are of the type $[Ru(bpy)_2(4\text{-methyl-}4'\text{-}(2\text{-arylethyl})\text{-}2,2'\text{-bipyridine})]^{2+}(ClO_4^-)_2$ where aryl = 2-naphthyl ([Ru]-naphthalene), 1-pyrenyl ([Ru]-pyrene), and 9-anthryl ([Ru]-anthracene). The overall yield of $MV^{\bullet+}$ is given by the product $\eta_q\eta_{ce}$, which depends both on specific solvent effects and on the nature of the quenched excited state of the bichromophore, i.e., whether it is a metal-to-ligand charge transfer (^{3}MLCT) or aromatic triplet state. In aqueous buffer the production of $MV^{\bullet+}$ is low for the three bichromophores (<10%). In methanol and acetonitrile $MV^{\bullet+}$ yields for [Ru]-anthracene and [Ru]-pyrene are >70%, reflecting the arene triplet character of the lowest excited state. This increase is due to an increase in the cage-escape efficiency (η_{ce}) in these solvents. In contrast, for [Ru]-naphthalene the lowest excited state is ^{3}MLCT in character and the yield of $MV^{\bullet+}$ in acetonitrile and methanol remains <10%. NMR spectra of the linking ethane group suggest that the bichromophores adopt different conformations in the different solvents, which could lead to the observed differences in η_{ce}.

1. Introduction

The system comprising $Ru(bpy)_3^{2+}$ and methyl viologen (MV^{2+}) is one of the most thoroughly studied photoredox systems for the storage of solar energy.[1,2] In the simplest case bimolecular oxidative quenching (k_q) by MV^{2+} competes with the normal radiative (k_{rad}) and nonradiative (k_{nrad}) decay processes of the $Ru(bpy)_3^{2+}$ excited state (Scheme 1). This involves the following steps. The first step is diffusion (k_{diff}) of the triplet excited state $^3Ru(bpy)_3^{2+}$ and a ground-state MV^{2+} dication to form a contact pair within a solvent cage. This is followed by electron transfer from the $^3Ru(bpy)_3^{2+}$ excited state to the MV^{2+} dication to produce a charge-transfer pair of the type $\{Ru(bpy)_3^{3+}/MV^{\bullet+}\}$. The resulting charge-transfer pair can then either diffuse apart (k_{ce}) to give the solvent-separated redox products $Ru(bpy)_3^{3+}$ and $MV^{\bullet+}$ or undergo back-electron transfer (k_{bet}) within the solvent cage followed by separation to produce ground-state reactants. In the former case, the reduced $MV^{\bullet+}$ diffuses to a catalytic site where two electrons are combined with hydronium ions to produce dihydrogen (k_{rxn}). A sacrificial electron donor is then used to regenerate the $Ru(bpy)_3^{2+}$ photosensitizer. In the absence of sacrificial donors, the solvent-separated redox products eventually recombine to form the starting materials (k_{rec}). Properties that have made $Ru(bpy)_3^{2+}$ and its derivatives the photosensitizer of choice for studying photoinduced electron transfer reactions include their strong absorption of solar radiation, their relatively long-lived excited states ($\tau \approx 1\ \mu$s), their favorable redox properties, and the fact that many of these properties can be "fine-tuned" by varying the number and composition of the complexing ligands.[3]

However, despite the favorable energetics of the system, the overall efficiency for dihydrogen production rarely exceeds 25% even in those cases where there is sufficient MV^{2+} to quench the photoexcited sensitizer quantitatively.[4−8] This is due to the fact that the overall quantum yield of $MV^{\bullet+}$ production (ϕ) depends on the product $\eta_{PS}{}^*\eta_q\eta_{ce}$. In this expression $\eta_{PS}{}^*$ is the quantum efficiency for the production of excited states (~1), η_q is the fraction of these that undergo electron-transfer quenching ($\eta_q = k_q[MV^{2+}]/(k_q[MV^{2+}] + k_{rad} + k_{nrad})$), and η_{ce} is the cage-escape efficiency of the redox pair ($\eta_{ce} = k_{ce}/(k_{ce} + k_{bet})$). At high quencher concentrations, η_{ce} is the rate-determining step and its magnitude is determined by the competition between cage escape of the redox pair, k_{ce}, and back-electron transfer within the solvent cage to regenerate the ground-state reactants, k_{bet}. We have previously shown that the intrinsically low cage-escape efficiency of this two-component system can be circumvented by incorporating an energy relay (anthracene-9-carboxylate, AA^-) into the scheme.[9,10] In this three-component system, the initially excited $^3Ru(bpy)_3^{2+}$ undergoes triplet−triplet energy transfer to AA^- to form $^3AA^-$

SCHEME 1

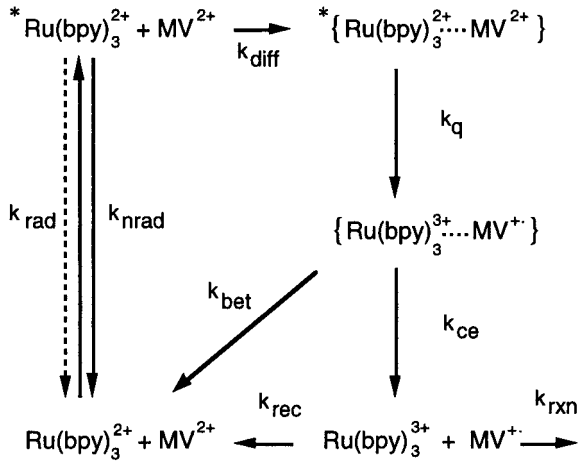

* To whom correspondence should be addressed. E-mail: Gerry.Wilson@MolSci.CSIRO.au.

S1089-5639(97)03248-9 CCC: $15.00
Published on Web 06/05/1998

with yields approaching 100%. $^3AA^-$ is then quenched by electron transfer to MV^{2+}, again with yields of up to 100%. Using this strategy, we have achieved quantum yields for hydrogen formation in excess of 85%. A mechanism that accounts for the high yields of $MV^{\bullet+}$ from this system has been proposed in which the cage-escape efficiencies are related to the degree of spin−orbit coupling in the geminate redox pair.[9−11] For the $\{Ru(bpy)_3^{3+}/MV^{\bullet+}\}$ charge-separated pair the spin multiplicity, which is initially triplet in character, quickly evolves singlet character due to spin−orbit coupling mediated by the internal heavy-atom effect of the ruthenium nucleus. As a consequence, the spin restriction for back-electron transfer is lifted, the rate of back-electron-transfer becomes comparable to the rate of cage escape of the redox products, and the yield of $MV^{\bullet+}$ is reduced. In contrast, for the $\{AA^{\bullet}/MV^{\bullet+}\}$ charge-separated pair the spin−orbit coupling is negligible and the original triplet character of the geminate pair is maintained. In this case, back-electron transfer to form ground-state products is formally spin-forbidden and, as we have shown, the cage-escape efficiency of the redox products can be quite high. More recent elaborations of this strategy have involved incorporating the energy relay chromophore (anthracene) directly onto the sensitizer using a flexible link consisting of either a $-CH_2-CH_2-$ or $-CH_2-O-CH_2-$ group.[12,13] It was then expected that the following sequence of reactions would occur, resulting in high yields of $MV^{\bullet+}$.

$$(bpy)_2Ru^{2+}(bpy\text{-}X\text{-}Anth) + h\nu \rightarrow (bpy)_2{}^3Ru^{2+}(bpy\text{-}X\text{-}Anth) \quad (1)$$

$$(bpy)_2{}^3Ru^{2+}(bpy\text{-}X\text{-}Anth) \xrightarrow{k_{ET}} (bpy)_2Ru^{2+}(bpy\text{-}X\text{-}{}^3Anth) \quad (2)$$

$$(bpy)_2Ru^{2+}(bpy\text{-}X\text{-}{}^3Anth) + MV^{2+} \xrightarrow{k'_{diff}} \{(bpy)_2Ru^{2+}(bpy\text{-}X\text{-}{}^3Anth)/MV^{2+}\} \quad (3)$$

$$(bpy)_2Ru^{2+}(bpy\text{-}X\text{-}{}^3Anth) \xrightarrow{k'_q} (bpy)_2Ru^{2+}(bpy\text{-}X\text{-}Anth^+)/MV^{\bullet+} \quad (4)$$

$$(bpy)_2Ru^{2+}(bpy\text{-}X\text{-}Anth^+)/MV^{\bullet+} \xrightarrow{k'_{bet}} (bpy)_2Ru^{2+}(bpy\text{-}X\text{-}Anth) + MV^{2+} \quad (5)$$

$$(bpy)_2Ru^{2+}(bpy\text{-}X\text{-}Anth^+)/MV^{\bullet+} \xrightarrow{k'_{ce}} (bpy)_2Ru^{2+}(bpy\text{-}X\text{-}{}^3Anth^+) + MV^{\bullet+} \quad (6)$$

where X = $-CH_2-CH_2-$ or $-CH_2-O-CH_2-$.

However, despite steps 1−3 proceeding quantitatively, the yields of $MV^{\bullet+}$ production are in most cases no different from the yields when the parent $Ru(bpy)_3^{2+}$ complex is used as the photosensitizer.[13] This is a surprising result, considering k'_{ce} should be much larger than k'_{bet}.

Given the unique energetics of the current series of bichromophores,[14,15] we have chosen to reexamine the quenching of $Ru(bpy)_3^{2+}$-linked arene systems in order to determine which processes are influential in determining the magnitude of $MV^{\bullet+}$ production.

2. Experimental Section

The synthesis of the perchlorate salts of the bichromophores has been described previously.[15] Spectroscopic grade solvents were used throughout, and solutions were thoroughly degassed by bubbling with purified argon prior to use. Absorption spectra were measured with a Cary-5E spectrophotometer, and emission spectra were measured with a Perkin-Elmer MPF-44 fluorimeter. In the steady-state quenching experiments the buildup of the methyl viologen radical cation ($MV^{\bullet+}$) versus time was monitored using an HP 8453 diode array spectrometer. Samples were irradiated in situ using a 150 W Xe lamp dispersed through a Bausch and Lomb monochromator (band-pass = 455 ± 10 nm). Since the rate of $MV^{\bullet+}$ production showed a dramatic solvent dependence, the intensity of the incident light (I_0) was adjusted with neutral density filters in order to control more accurately the irradiation dose. Changes in $MV^{\bullet+}$ were monitored at 605 nm and were corrected for the different values of I_0 and for the slightly different optical densities of the solutions at 455 nm (∼0.6). Irradiations were terminated when the optical density at 605 nm reached 0.1. Quenching experiments were carried out in acetate buffer (pH = 5.0) using ethylenediaminetetraacetic acid (EDTA) as the sacrificial donor and in acetonitrile, methanol, and water (pH = 10) using triethylamine (TEA) as the sacrificial donor. For luminescent donors Stern−Volmer quenching constants (K_{SV}) were determined from plots of both (τ_0/τ_q) and (I_0/I_q) versus $[MV^{2+}]$. For [Ru]-anthracene, which is nonemitting, K_{SV} was determined from plots of the intensity and/or lifetime of the anthracene triplet−triplet absorption signal measured at 420 nm versus $[MV^{2+}]$. Procedures for measuring the transient absorption spectra and decays have been given previously.[15] ^1H NMR data were measured with a Bruker Avance DRX 500 MHz spectrometer.

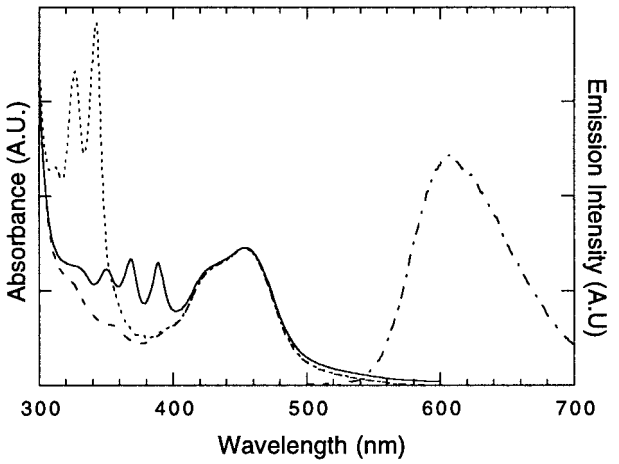

Figure 1. Absorption spectra of [Ru]-naphthalene (- - -), [Ru]-pyrene (•••), and [Ru]-anthracene (−) and the emission spectrum of [Ru]-Pyrene (-•-) in degassed methanol.

3. Results

The absorption spectra of the bichromophores in methanol are shown in Figure 1. In each case the absorption spectrum of the bichromophore complex is indistinguishable from the sum of the spectra of its individual component chromophores. In Figure 1 this is seen most clearly in the case of [Ru]-pyrene and [Ru]-anthracene, which have distinctive absorption features due to the pendant aryl group in the near-UV region. In the case of [Ru]-naphthalene the effect is most noticeable in the region of the strong ^1B_b naphthalene absorption between 200 and 250 nm. The emission spectrum of [Ru]-pyrene is also shown in Figure 1. The emission spectra of both [Ru]-naphthalene and [Ru]-pyrene are similar to that of $Ru(bpy)_3^{2+}$

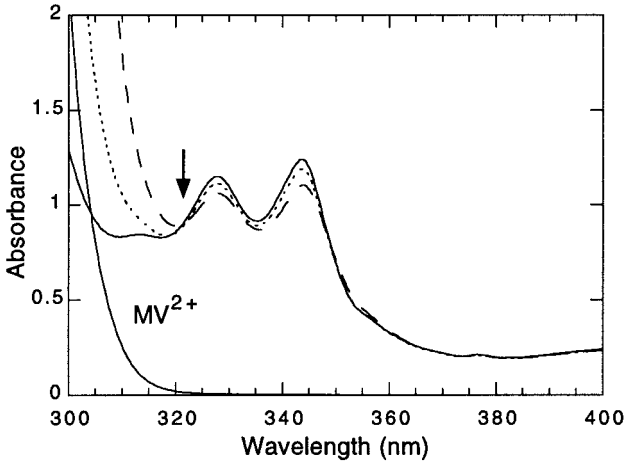

Figure 2. Effect of added MV^{2+} on the absorption spectrum of [Ru]-pyrene: neat [Ru]-pyrene in water (−); 2×10^{-3} M added MV^{2+} (···); 8×10^{-3} M (- - -) added MV^{2+}. Absorption spectrum of an 8×10^{-3} M solution of MV^{2+} (−). The isosbestic point is indicated by an arrow.

($\lambda_{max} = 605$ nm). Excitation spectra[15] monitored at the emission maximum matched the absorption spectra. In contrast to the other two bichromophores, [Ru]-anthracene is nonemitting at room temperature, although anthracene phosphorescence is clearly observed at low temperatures (77 K).[15] The effects of adding different amounts of MV^{2+} to the absorption spectrum of an aqueous solution of [Ru]-pyrene are shown in Figure 2. Also included for comparison is the absorption spectrum of MV^{2+}.

The steady-state production of $MV^{\bullet+}$ versus irradiation time for solutions containing [Ru]-naphthalene, [Ru]-pyrene, [Ru]-anthracene, and $Ru(bpy)_3^{2+}$ in water at pH 5 using EDTA as sacrificial donor is shown in Figure 3a. Qualitatively similar results were obtained in aqueous solutions at pH $\approx$ 10 using TEA as the sacrificial donor. The results of analogous experiments obtained using methanol as solvent are shown in Figure 3b. In these experiments the concentration of the photosensitizer was adjusted to give an optical density of 0.6 at the excitation wavelength (455 nm), which corresponded to a photosensitizer concentration of $\sim 3 \times 10^{-5}$ M. The concentrations of the electron acceptor (MV^{2+}) and sacrificial donor (TEA) were kept fixed at 2×10^{-3} and 2×10^{-2} M, respectively. The results of steady-state quenching experiments in acetonitrile were quantitatively similar to those obtained in methanol.

To check that the production of $MV^{\bullet+}$ in the different solvents was not simply due to the relative electron-transfer efficiencies of the different sacrificial donors, time-resolved production of $MV^{\bullet+}$ was measured for aerated solutions in the absence of sacrificial donors. Typical time-resolved absorption profiles for $MV^{\bullet+}$ following photoexcitation of [Ru]-pyrene in water and methanol are shown in Figure 4. The production of $MV^{\bullet+}$ for an aqueous solution of $Ru(bpy)_3^{2+}$ is also shown for comparison. In these experiments, the photosensitizer concentrations were adjusted to give the same optical densities at the excitation wavelength (350 nm) and the absorption of $MV^{\bullet+}$ was probed with a helium−neon laser at 633 nm. The solid lines in Figure 4 are single-exponential fits of the decays at 633 nm and are shown as a visual aid only. In the absence of sacrificial donors the decay of $MV^{\bullet+}$ will depend on the efficiency of charge recombination for the geminate ion pair (and hence their concentration) and also on the amount of dissolved oxygen in the solution. As a result, in the absence of sacrificial donors the decay of $MV^{\bullet+}$ is expected to show a complex time dependence. In any event the relevant information from Figure

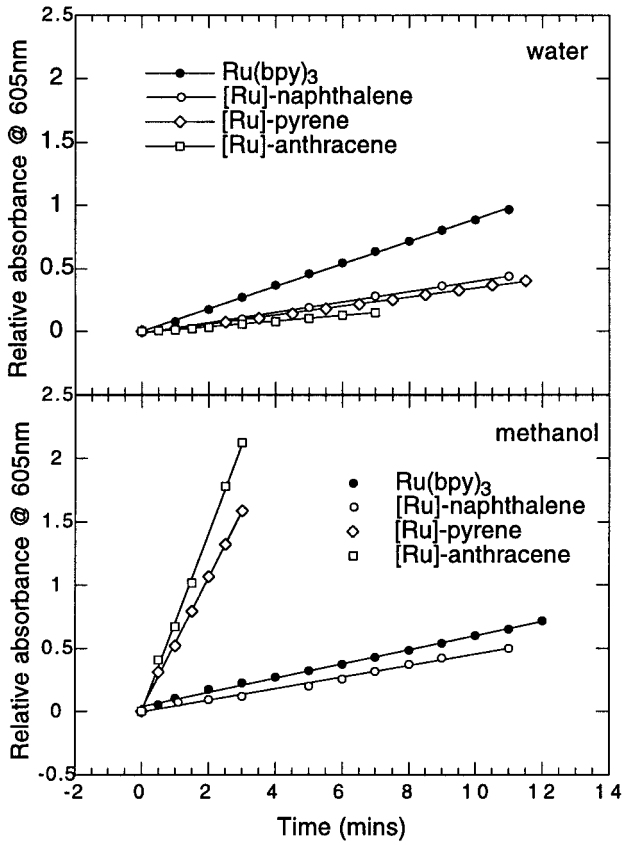

Figure 3. Steady-state production of $MV^{\bullet+}$ versus irradiation time for (a, top) $\lambda_{exc} = 455$ nm and (b, bottom) $\lambda_{obs} = 605$ nm. See text for details of sensitizer and quencher concentrations.

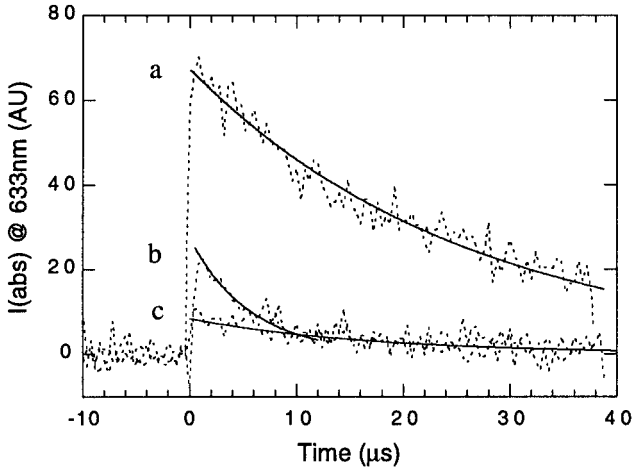

Figure 4. Time-resolved production of $MV^{\bullet+}$ vs time for (a) [Ru]-pyrene in methanol, (b) $Ru(bpy)_3^{2+}$ in water, and (c) [Ru]-pyrene in water. The transient absorption of $MV^{\bullet+}$ (broken lines) was monitored at 633 nm. The solid lines are single-exponential fits of the decays.

4 are the intensities at time zero, which we use to confirm the steady-state production yields of $MV^{\bullet+}$.

In the case where the excited-state donor is luminescent, the quenching constant k_q is determined from the Stern−Volmer relationship:

$$\frac{I_0}{I_q} \text{ or } \left(\frac{\tau_0}{\tau_q}\right) = 1 + \frac{k_q[MV^{2+}]}{k_{rad} + k_{nrad}}$$

$$= 1 + K_{SV}[MV^{2+}] \qquad (7)$$

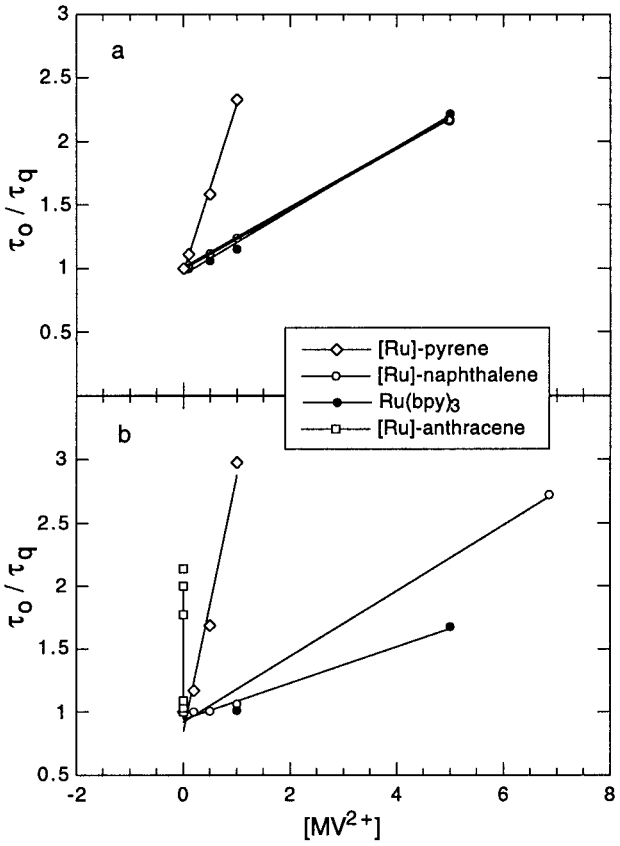

Figure 5. Stern-Volmer plots of the bichromophores in (a) water and (b) methanol.

where I_0 (τ_0), I_q (τ_q) are the emission intensity (lifetime) in the absence and presence of the quencher, respectively, and K_{SV} is the Stern−Volmer quenching constant. The quenching rate k_q can then be determined from

$$k_q = \frac{K_{SV}}{\tau_0} \tag{8}$$

Representative Stern−Volmer plots for the bichromophores in water and methanol are shown in parts a and b of Figure 5, respectively.

In the case of the nonluminescent [Ru]-anthracene, a similar treatment of either the intensity or the lifetime of the transient absorption signal monitored at 425 nm provides values for K_{SV} and k_q. The fraction η_q of excited-state donors that are quenched can then be determined from the relationship

$$\eta_q = \frac{k_q[MV^{2+}]}{k_{rad} + k_{nrad} + k_q[MV^{2+}]} = \left(1 + \frac{1}{K_{SV}[MV^{2+}]}\right)^{-1} \tag{9}$$

Under conditions of steady-state illumination and in the presence of a sacrificial electron donor such as EDTA, $Ru(bpy)_3^{3+}$ is reduced back to the starting material and the concentration of the methyl viologen radical cation in solution increases (Figure 3). The rate of production of $MV^{\bullet+}$ therefore depends on the product $\eta_{PS}{}^*\eta_q\eta_{ce}$. By comparing the initial slopes for the linked bichromophores (unprimed values) with that obtained for $Ru(bpy)_3^{2+}$ (primed values) under otherwise identical conditions, η_{ce} for the linked bichromophores can be evaluated.[13] In eq 10, values for η_q were obtained from K_{SV} (eq 9) and values for η_{ce}' in the different solvents were 0.26 (water),[7] 0.25, (buffer),[7] and 0.27 (methanol).[11]

$$\eta_{ce} = \frac{(\text{slope})\eta_q'\eta_{ce}'}{(\text{slope}')\eta_q} \tag{10}$$

The primed values in eq 10 refer to $Ru(bpy)_3^{2+}$, and the unprimed values refer to the bichromophores. The derived rate constants and cage-escape yields are given in Table 1.

The ^1H NMR spectra of the ethane linking group in [Ru]-pyrene measured in deuterated water, methanol, and dichloromethane are shown in Figure 6.

4. Discussion

Despite the size of the spacer group, there is little, if any, ground-state interaction between the constituent parts of the bichromophores as evidenced by the similarity between the absorption spectra of the complexes and the absorption spectra of the component chromophores. Previously, we have shown that the photophysical processes of these bichromophores are determined by the relative positions of the various singlet and triplet energy levels.[14,15] For [Ru]-naphthalene, the excitation energy is localized entirely on the [Ru]-centered ^{3}MLCT state, whereas for [Ru]-anthracene, the excitation energy is localized on the anthracene triplet state. Consequently, the excited states that are ultimately quenched in the experiments reported here can be described as ^{3}[Ru]*-naphthalene and [Ru]-^{3}anthracene*, respectively. In the special case of [Ru]-pyrene, the ^{3}MLCT and the lowest pyrene triplet state are in equilibrium and the excitation energy is localized approximately 15% on the [Ru]-centered ^{3}MLCT state with the remaining 85% localized on the pyrene triplet state. In principle, therefore, quenching of [Ru]-pyrene can involve the participation of either the [Ru]-centred ^{3}MLCT state or the pyrene triplet state.

The increase in size in replacing the pendant naphthalene chromophore by either an anthracene or a pyrene is relatively small in terms of the overall structure of these bichromophores. Similarly, the solubilities of the three aromatic chromophores in the different solvents are not expected to be too different. We therefore expect solvation effects and other intermolecular interactions (e.g., effects of counterions, spectator ions, solvent, etc.) to be similar for the three bichromophores. Furthermore, any major differences in their quenching behavior should reflect differences in their energetics. As a result, this series provides a good opportunity to examine the relative quenching efficiencies of ^{3}MLCT and the aromatic triplet states by MV^{2+} as well as the role of spin−orbit coupling on the cage escape yield of $MV^{\bullet+}$.

Quenching in Acetate Buffer. The overall yield of $MV^{\bullet+}$ ($\phi_{MV^{\bullet+}} = \eta_q\eta_{ce}$) for [Ru]-naphthalene, [Ru]-pyrene, and [Ru]-anthracene in acetate buffer is uniformly low (∼5%). From a solar energy conversion perspective, this is a rather disappointing result, since it means that the yield of hydrogen production from the photoreduction of water would be greatly reduced using these photosensitizers compared with that of the model system of $Ru(bpy)_3^{2+}$ and MV^{2+} (where $\eta_q\eta_{ce} \approx 25\%$).[4−8] It is also a somewhat surprising result, considering the character of the quenched excited states of the bichromophores is quite different. Consequently, it is instructive to compare the relative contributions of η_q and η_{ce} to the overall yield of $MV^{\bullet+}$ for the different systems (Table 1). Considering first the quenching efficiencies (η_q), it can be seen that the systems involving ^{3}MLCT excited states (i.e., [Ru]-naphthalene and $Ru(bpy)_3^{2+}$) have consistently lower quenching efficiencies than those involving predominantly the aromatic triplet state, e.g., [Ru]-pyrene. A possible exception to this trend is the value of η_q observed for [Ru]-anthracene, which is considerably lower than what one would expect on

TABLE 1: Quenching Data for the Bichromophores and the Model Complex in Different Solvents

complex	solvent	K_{SV}, L mol^{-1}	τ_0, μs	k_q ($\times 10^9$) L mol^{-1} s^{-1}	d[MV$^{\bullet+}$]/dt	η_q	η_{ce}	$\eta_q\eta_{ce}$
Ru(bpy)$_3$	buffer[a]	615	0.640	0.96	0.090	0.55	0.25[c]	0.14
	water[b]	296	0.593	0.50	0.136	0.37	0.26[c]	0.10
	methanol	210	0.667	0.31	0.060	0.30	0.27[d]	0.08
[Ru]-naphthalene	buffer	698	0.530	1.32	0.042	0.58	0.11	0.06
	water	240	0.525	0.46	0.096	0.38	0.18	0.07
	methanol	260	0.785	0.33	0.055	0.34	0.22	0.07
[Ru]-pyrene	buffer	3630	2.175	1.67	0.037	0.88	0.065	0.06
	water	1325	2.058	0.64	0.093	0.72	0.09	0.06
	methanol	2027	4.940	0.41	0.523	0.80	0.88	0.70
[Ru]-anthracene	buffer	705	230.0	0.003	0.024	0.58	0.06	0.03
	methanol	$>10^5$	350.0	0.28	0.705	0.99	0.96	0.95

[a] Acetate buffer, sacrificial donor = EDTA, pH = 5. [b] Sacrificial donor = TEA, pH = 10. [c] Reference 7. [d] Reference 11.

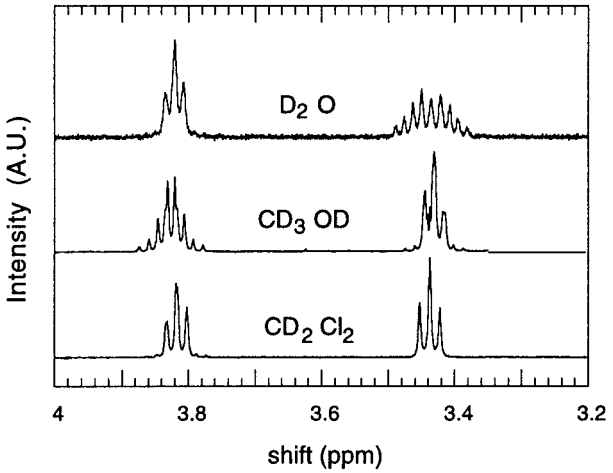

Figure 6. ^{1}H NMR spectra of for [Ru]-pyrene in (a) D_2O and (b) CD_3OD.

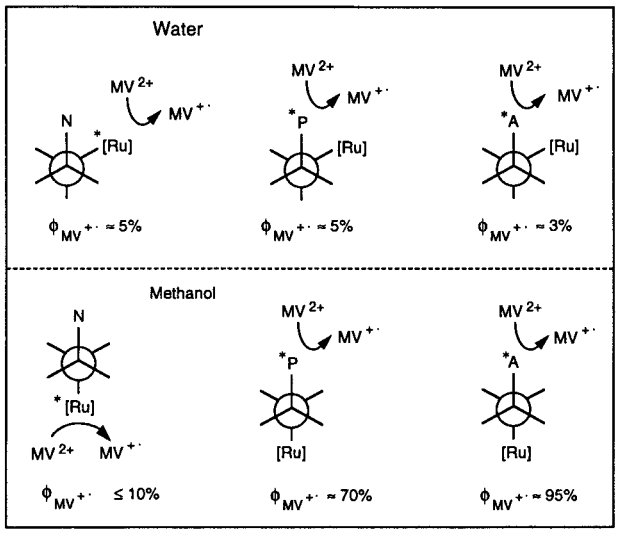

Figure 7. Schematic representation of the quenching process in different solvents.

the basis of its aromatic triplet-state character. Since K_{SV} for [Ru]-anthracene was determined from quenching of the anthracene triplet−triplet absorption spectrum (which has large associated experimental errors), there is a correspondingly large uncertainty in the determination of K_{SV}. Consequently, we believe that the actual quenching efficiency, η_q, for [Ru]-anthracene is closer to 90%.

If we now consider the cage-escape efficiency (η_{ce}) in acetate buffer, we see that there is a large decrease in η_{ce} for the bichromophores compared with η_{ce} of the model system Ru(bpy)$_3^{2+}$/MV^{2+}. Once again, this change is most noticeable for systems where the quenched species is an aromatic triplet state. In this case, the cage-escape yields for [Ru]-anthracene and [Ru]-pyrene decrease by a factor of 4 compared with that of the model system. Unfortunately, this reduction in η_{ce} is more than enough to overcome the increase observed in η_q for these systems, and as a result, the overall yield of MV$^{\bullet+}$ for [Ru]-anthracene and [Ru]-pyrene in acetate buffer is a disappointingly low 5%. In the case of [Ru]-naphthalene, which, like the model compound, has a ^{3}MLCT lowest excited state, the decrease in the cage escape yield is not as dramatic. In this case η_{ce} decreases by a factor of 2 compared with the model system. However, when combined with its inherently low quenching efficiency, the overall production yield of MV$^{\bullet+}$ for [Ru]-naphthalene in acetate buffer is also rather low, ~5%. To summarize, although the overall yields of MV$^{\bullet+}$ for the three bichromophores are very similar, this similarity arises from the fortuitous combination of η_q and η_{ce} to $\phi_{MV^{\bullet+}}$, which is based on the different properties of the ^{3}MLCT and aromatic triplet states.

We believe the quenching behavior of the bichromophores is the result of two separate effects. The first effect involves a conformational change in the bichromophores. This arises from the minimization of unfavorable hydrophobic interactions between the pendant aromatic chromophores and hydrophilic solvents. As a result, the bichromophores adopt different conformations in different solvents. This is shown schematically in Figure 7. Taking [Ru]-pyrene as an example, if the bichromophore were to prefer a conformation in which the [Ru] center and the pyrene chromophore are anti- with respect to the linking ethane group, then, to a first approximation, the methylene protons of the ethane group should experience similar chemical environments. The region of the NMR spectrum featuring the methylene protons of the spacer group for [Ru]-pyrene in deuterated water, methanol, and dichloromethane is shown in Figure 6. In dichloromethane a symmetrical splitting pattern consisting of two triplets is observed, indicating the near equivalence of the methylene protons. It appears that in this solvent the bichromophore prefers an "extended" anti conformation. This is also in agreement with its high solubility in this solvent. The methylene proton splitting pattern gets progressively more complicated as the solvent is changed. In methanol the triplet centered at 3.82 ppm becomes a multiplet of eight peaks, whereas in deuterated water the triplet at 3.44 ppm becomes a multiplet of nine peaks. As a result, we conclude that different rotamers of the bichromophore are favored in different solvents. Analogous NMR spectra were obtained for [Ru]-naphthalene in the same solvents. The second effect

contributing to the overall quenching behavior of the bichromophores is the formation (in acetate buffer) of a weak ground-state complex between the bichromophores and MV^{2+}. Again, taking [Ru]-pyrene as an example, we observe a distinct change in the absorption spectrum of [Ru]-pyrene following the addition of MV^{2+} (Figure 2). The pyrene absorption band at 337 nm decreases and broadens slightly, and an intense new band/shoulder appears below 320 nm. An isosbestic point associated with these changes is also observed at 323 nm. We attribute these spectral changes to the formation of a weak ground-state complex between the methyl viologen dication and the pendant aromatic group in the bichromophore. Similar (albeit weaker) spectral changes are observed for [Ru]-anthracene. We were unable to identify analogous changes in the absorption spectrum of [Ru]-naphthalene presumably because of the weak absorption of the naphthalene chromophore at wavelengths greater than 310 nm. Since no change to the $Ru(bpy)_3^{2+}$ absorption spectrum has been reported for solutions of $Ru(bpy)_3^{2+}$ and MV^{2+}, it appears that the presence of an aromatic chromophore is necessary for such complexation to occur. Work is currently in progress to determine the importance of factors such as spacer length and flexibility on ground-state complexation and its subsequent effect on quenching processes of the bichromophores.

As expected, the formation of ground-state complexes results in enhanced yields of quenching for bichromophores having lowest excited states that are localized on the aromatic chromophore (i.e., [Ru]-pyrene and [Ru]-anthracene) (Table 1). However, this increase in the quenching efficiency cannot be fully exploited owing to the conformational constraints described above. In aqueous acetate buffer it appears that the aromatic chromophores are in a conformation that brings them close to the ruthenium center owing to the unfavorable hydrophobic interactions (Figure 7). As a result, during the quenching process the aromatic triplet state and MV^{2+} are sufficiently close to the ruthenium center for it to affect the spin−orbit coupling of the redox pair. Since the redox pair initially has triplet character, back-electron transfer is formally spin-forbidden. However, spin−orbit coupling induced by the heavy ruthenium nucleus lifts the spin restriction to back-electron transfer, and as a result, the rate of back-electron transfer increases and there is a concomitant decrease in the cage-escape yield (Scheme 1). In the case of [Ru]-naphthalene η_q was also found to decrease with respect to the parent complex. In this case the increase in hydrophobicity of the bichromophore due to the proximity of the pendant aromatic hydrocarbon might induce the viologen radical cation to remain longer within the geminate-pair solvent cage. This could be due either to a specific $MV^{\bullet+}$/naphthalene interaction or to the solubility of $MV^{\bullet+}$ in the different solvents. In either case, increasing the lifetime of the geminate ion pair increases the chances of back-electron transfer occurring, which in turn decreases the production of $MV^{\bullet+}$.

Quenching in Methanol and Acetonitrile. An entirely different type of behavior is observed for the bichromophores in organic solvents such as methanol and acetonitrile. First, the NMR spectra of the bichromophores in these solvents are quite different from those measured in aqueous solvents (Figure 6). Furthermore, the bichromophores are also considerably more soluble in these solvents than in aqueous buffer. We interpret this to mean that in methanol and acetonitrile the bichromophores prefer conformations that tend to maximize the distance between the two chromophores; i.e., they prefer a more "extended" or "anti"-like structure. As a result, quenching of the different excited states should take place relatively independently of the adjacent chromophore. This is shown schematically in Figure 7.

SCHEME 2

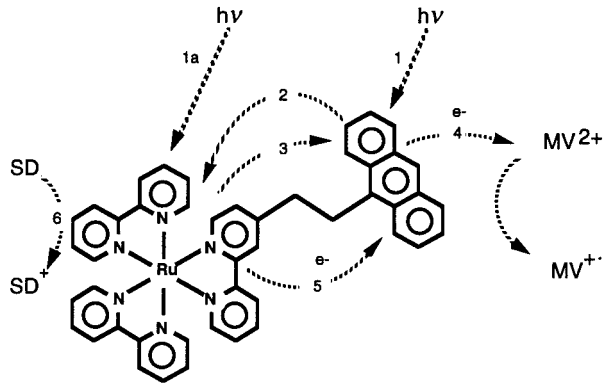

Considering the ^{3}MLCT nature of their excited states, it is not surprising to find that both [Ru]-naphthalene and $Ru(bpy)_3^{2+}$ have very similar quenching and cage-escape efficiencies in methanol and acetonitrile. This is due to the more extended structure of [Ru]-naphthalene in methanol, which allows the [Ru]-centered ^{3}MLCT state to be quenched with minimal influence from the tethered naphthalene group. The result is an increase by a factor of 2 in the cage-escape efficiency for [Ru]-naphthalene in methanol compared with that in buffer solution. The small differences between [Ru]-naphthalene and $Ru(bpy)_3^{2+}$ are possibly due to minor steric and/or shielding effects of the pendant naphthalene chromophore. However, for both these complexes the moderate values observed for η_q and η_{ce} result in an overall value for $\phi_{MV^{\bullet+}}$ that is still quite low, <10%. It is also worth noting that even if the cage-escape yields were quantitative, the overall yield of $MV^{\bullet+}$ would not exceed ~30% in either of these systems. This low yield of cage-escape for the geminate pairs is in agreement with earlier work on other ^{3}MLCT-based systems.[1] The situation is quite different when the excitation is localized either fully or partially on the aromatic chromophore. In this case both the quenching efficiencies and the cage-escape yields are high (~90%). Not surprisingly, the highest combined yield was found for [Ru]-anthracene where the excitation is fully localized on the long-lived anthracene triplet state. In this case the ion pair undergoes both quenching and cage escape with almost unit efficiency to produce $MV^{\bullet+}$ in yields of approximately 95%. For [Ru]-pyrene on the other hand, about 15% of the initial excitation energy is localized on the $Ru(bpy)_3^{2+}$ moiety. This lowers the overall yield of $\phi_{MV^{\bullet+}}$, since both the overall quenching of the ^{3}MLCT state, which is inherently low (<10%), and the radiative and nonradiative processes associated with the ^{3}MLCT tend to act as a nonproductive funnel back to the ground state. As a result, η_q for [Ru]-pyrene is ~80% compared with ~100% for [Ru]-anthracene and the overall yield of $MV^{\bullet+}$ for [Ru]-pyrene is reduced to ~70%. No evidence was found for any ground-state complexation between the bichromophores and $MV^{\bullet+}$ in these solvents. In this case the large increase in η_q for these systems is attributed to the lifetime of the aromatic triplet state, which for [Ru]-^{3}pyrene is 4.94 μs and for [Ru]-^{3}anthracene is 350 μs. Finally, using time-resolved absorption spectroscopy, we have been unable to observe the radical cations of either anthracene or pyrene at any time following the laser pulse during quenching of these bichromophores. To summarize, for [Ru]-anthracene, quenching of the bichromophore in methanol involves the following sequence of events (Scheme 2). Pho-

toexcitation of the aromatic chromophore (step 1) produces the excited singlet state, which undergoes extremely rapid singlet−singlet energy transfer (k_{ET}^{s-s}) to the [Ru] center with close to unit quantum yield (step 2). This is followed by intersystem crossing to the ^{3}MLCT state, again, with unit quantum yield. The alternative pathway for ^{3}MLCT formation involves direct excitation of the [Ru]-centered ^{1}MLCT state[1] followed by intersystem crossing to the ^{3}MLCT state. In either case the ^{3}MLCT state thus formed undergoes triplet−triplet energy transfer (step 3) back to the aromatic chromophore (k_{ET}^{t-t}) to produce the anthracene triplet state. The efficient production of the anthracene triplet state by this process is the reason that [Ru] anthracene is nonemitting. The resulting anthracene triplet state is long-lived (350 μs) and undergoes efficient intermolecular electron-transfer quenching by MV^{2+} (k_{ET}^{inter}) (step 4). In the absence of any spectroscopic evidence for the formation of the anthracene radical cation, we conclude that intermolecular electron transfer to MV^{2+} is immediately followed by rapid intramolecular electron transfer (k_{ET}^{intra}) within the bichromophore (step 5), which regenerates ground-state anthracene and produces $Ru(bpy)_3^{3+}$. $Ru(bpy)_3^{3+}$ is subsequently reduced (step 6) back to $Ru(bpy)_3^{2+}$ through bimolecular quenching by the sacrificial electron donor (TEA or EDTA).

5. Conclusions

The efficiency of photooxidative quenching of [Ru]-naphthalene, [Ru]-pyrene, and [Ru]-anthracene by MV^{2+} depends on the nature of the excited state (i.e., whether they are MLCT or aromatic triplet in nature) and on the type of solvent. The solvent effect is caused by (i) conformational changes brought about by the minimization of unfavorable chromophore/solvent interactions and (ii) the formation, in aqueous buffer, of a weak solute/quencher complex. For bichromophores where the lowest excited state is MLCT in character, the production efficiency of $MV^{\bullet+}$ is always $<10\%$ irrespective of the solvent. This is a reflection of the low quenching and cage-escape efficiencies of the redox pair. In contrast, where the lowest excited state is an aromatic triplet state, the production efficiency of $MV^{\bullet+}$ can be as high as 100% in organic solvents. When the excitation energy is in equilibrium between the excited states, the efficiency of $MV^{\bullet+}$ production reflects the partitioning of the excitation energy between the two states.

Acknowledgment. The authors thank P. Gurr for careful synthesis of some of the ligands and I. Willing for NMR analysis of the complexes.

References and Notes

(1) Kalyanasundaram, K. *Coord. Chem. Rev.* **1982**, *46*, 159.
(2) Meyer, T. J. *Prog. Inorg. Chem.* **1983**, *30*, 389.
(3) Juris, A.; Barigelletti, F.; Campagna, S.; Balzani, V.; Belser, P.; Von Zelewsky, A. *Coord. Chem. Rev.* **1988**, *84*, 85.
(4) Kalyanasundaram, K.; Kiwi, J.; Gratzel, M. *Helv. Chim. Acta* **1978**, *61*, 2720.
(5) Maestri, M.; Sandrini, D. *Nouv. J. Chim.* **1981**, *5*, 637.
(6) Chan, S.-F.; Chou, M.; Creutz, C.; Matsuhara, T.; Sutin, N. *J. Am. Chem. Soc.* **1981**, *103*, 369.
(7) Kalyanasundaram, K.; Neuman-Spallart, M. *Chem. Phys. Lett.* **1982**, *88*, 7.
(8) Mandal, K.; Hoffman, M. Z. *J. Phys. Chem.* **1984**, *88*, 185.
(9) Johansen, O.; Mau, A. W.-H.; Sasse, W. H. F. *Chem. Phys. Lett.* **1983**, *94*, 107.
(10) Johansen, O.; Mau, A. W.-H.; Sasse, W. H. F. *Chem. Phys. Lett.* **1983**, *94*, 113.
(11) Olmsted, J., III; Meyer, T. J. *J. Phys. Chem.* **1987**, *91*, 1649.
(12) Boyde, S.; Strouse, G. F.; Jones, W. E., Jr.; Meyer, T. J. *J. Am. Chem. Soc.* **1989**, *111*, 7448.
(13) Weinheimer, C.; Choi, Y.; Caldwell, T.; Gresham, P.; Olmsted, J., III. *J. Photochem. Photobiol., A* **1994**, *78*, 119.
(14) Wilson, G. J.; Sasse, W. H. F.; Mau, A. W.-H. *Chem. Phys. Lett.* **1996**, *250*, 583.
(15) Wilson, G. J.; Launikonis, A.; Sasse, W. H. F.; Mau, A. W.-H. *J. Phys. Chem. A* **1997**, *101*, 4860.